Broadband ferromagnetic resonance characterization of anisotropies and relaxation in exchange-biased IrMn/CoFe bilayers

Jamileh Beik Mohammadi,[1,2,*] Joshua Michael Jones,[1,2] Soumalya Paul,[1,2] Behrouz Khodadadi,[1,2] Claudia K. A. Mewes,[1,2] Tim Mewes,[1,2] and Christian Kaiser[3]

[1]*Center for Materials for Information Technology, University of Alabama, Tuscaloosa, Alabama 35487, USA*

[2]*Department of Physics and Astronomy, University of Alabama, Tuscaloosa, Alabama 35487, USA*

[3]*Western Digital, Fremont, California 94539, USA*

(Received 9 November 2016; published 15 February 2017)

The magnetization dynamics of exchange-biased IrMn/CoFe bilayers have been investigated using broadband and in-plane angle-dependent ferromagnetic resonance spectroscopy. The interface energy of the exchange bias effect in these bilayers exceeds values previously reported for metallic antiferromagnets. A strong perpendicular magnetic anisotropy and a small in-plane uniaxial anisotropy are also observed in these films. The magnetization relaxation of the bilayers has a strong unidirectional contribution, which is in part caused by two-magnon scattering. However, a detailed analysis of in-plane angle– and thickness-dependent linewidth data strongly suggests the presence of a previously undescribed unidirectional relaxation mechanism.

DOI: 10.1103/PhysRevB.95.064414

I. INTRODUCTION

Since the discovery of the exchange bias effect by Meiklejohn and Bean in 1956 [1,2], this topic has remained a very active research area. This is due in part to the many practical applications of this effect in data storage devices. In recent years, the exchange bias effect has been of particular importance for pinning the reference layer in spin valve structures [3], which are used, for example, in read heads and spin transfer torque magnetic random access memories [4,5]. Another reason for the continued interest in this topic is the inherent complexity of the competing interactions at the interface between a ferromagnet and an antiferromagnet [6], which leads to very rich physics [7]. A particularly interesting feature, not only for future applications, but also for obtaining new insights into the underlying physics, is the influence of the exchange bias effect on the magnetization dynamics of the ferromagnet [8,9]. One of the most prominent features of the exchange bias effect is that it leads to a preferred direction of the magnetization (unidirectional anisotropy) of the bilayer system. This easy direction of the unidirectional anisotropy is typically established during annealing and subsequent cooling in an applied magnetic field. The unidirectional anisotropy manifests itself in a shift or "bias" of the magnetization reversal curve on the magnetic field axis. However, magnetization reversal measurements can be difficult to analyze quantitatively, in particular, due to the complex phase diagrams [10,11] and the formation of complicated domain structures [12–15]. Here, measurements of the magnetization dynamics, for example, using ferromagnetic resonance [8,16–18] or Brillouin light scattering [17–19], offer the advantage that they can be carried out at external magnetic fields sufficient to saturate the system. While most of the early work on magnetization dynamics of exchange-biased systems focused on the determination of the unidirectional anisotropy to provide input to model development, it was also noted early on that the exchange bias effect has a profound influence on the magnetization relaxation in these systems [16,18]. Two-magnon scattering at the ferromagnet/antiferromagnet interface is one of the major contributions to the relaxation in these systems [9,17,20]. However, it was only after the development of broadband ferromagnetic resonance capabilities that a unidirectional contribution to the relaxation in these systems was observed [21].

In the present paper, we utilize broadband ferromagnetic resonance to investigate the magnetization dynamics in the IrMn/CoFe exchange-biased system to precisely determine anisotropies. By investigating the CoFe thickness and in-plane angle dependencies, we are able to show that this system has a strong interfacial perpendicular anisotropy in addition to the very strong interfacial exchange coupling. We further show that the magnetization relaxation in this system has a very strong unidirectional contribution, which is in part caused by two-magnon scattering. However, we also present evidence that the strong unidirectional relaxation in this system deviates from the expected thickness dependence of a strictly interfacial two-magnon scattering contribution. Our analysis therefore suggests the presence of a previously undescribed unidirectional relaxation mechanism in this system.

The paper is organized as follows. In Sec. II, we describe the experimental procedures used to characterize the samples. In Sec. III, we summarize the models commonly used to describe ferromagnetic resonance in exchange-biased systems. Section IV describes the results regarding the magnetic anisotropies present in the IrMn/CoFe exchange-biased system. In Sec. V, we describe in detail the results regarding the strong unidirectional magnetization relaxation observed in this system. The paper concludes with a summary in Sec. VI.

II. EXPERIMENTAL PROCEDURES

The samples were prepared with an Anelva sputter deposition system onto SiO_2 substrates with the following layer sequence: SiO_2/Ta (2 nm)/Ru (3 nm)/IrMn (6 nm)/CoFe (t)/Ru (3 nm)/Ta (2 nm)/Ru (5 nm). The

*Corresponding author: jbeikmohammadi@crimson.ua.edu

CoFe layer thickness t ranged from 2 to 20 nm. In order to set the exchange bias direction, the samples were annealed at 285 °C for 5 hours in an applied field of 5 T. The IrMn thickness of 6 nm is significantly larger than the critical thickness of this antiferromagnet, thereby ensuring saturation of the exchange bias effect [22].

The quasistatic magnetic properties of the samples were determined using magneto-optical Kerr effect (MOKE) measurements, whereas the dynamic properties were determined using broadband ferromagnetic resonance spectroscopy (FMR) covering a frequency range from 2 to 64 GHz. In both cases, the samples were measured at room temperature.

For broadband FMR measurements, the external field was oriented parallel and antiparallel to the exchange bias direction. In addition, we also carried out in-plane angle–dependent measurements at selected frequencies to obtain additional information about the magnetic anisotropies and the relaxation mechanisms of the samples. The raw spectroscopy data were analyzed by fitting a Lorentzian peak profile including both dispersive and absorptive components in order to extract the resonance field, $H_{\rm res}$, and the peak-to-peak linewidth, ΔH, at each frequency [23,24].

III. FERROMAGNETIC RESONANCE IN AN EXCHANGE BIAS SYSTEM

In FMR measurements, the resonance condition can be derived using the Smit and Beljers relation [25]:

$$\left(\frac{\omega}{\gamma}\right)^2 = \frac{1}{M_s \sin^2\theta}\left[\frac{\partial^2 F}{\partial\theta^2}\frac{\partial^2 F}{\partial\phi^2} - \left(\frac{\partial^2 F}{\partial\theta\,\partial\phi}\right)^2\right] \quad (1)$$

where $\omega = 2\pi f$ is the angular frequency of the microwave field, M_s is the saturation magnetization, γ is the gyromagnetic ratio, θ is the polar angle of the magnetization with respect to the normal of the film, and ϕ is the azimuthal angle of the magnetization, for which we chose the exchange bias direction as a reference, i.e., $\phi_{eb} = 0$ (see Fig. 1). The free energy F of the ferromagnet in the exchange bias system includes Zeeman, demagnetizing, exchange bias, and uniaxial anisotropy terms. The last two contributions are characterized by the exchange bias field H_{eb} and the uniaxial anisotropy field $H_u = \frac{2K_u}{M_s}$.

Equation (1) is evaluated at the equilibrium (θ_0,ϕ_0) of the magnetization for which

$$\left.\frac{\partial F}{\partial\theta}\right|_{\theta_0} = 0, \text{ and } \left.\frac{\partial F}{\partial\phi}\right|_{\phi_0} = 0 \quad (2)$$

In its most general form, Eq. (3) does not have an analytical solution, but it can be readily solved numerically. To obtain further insights, analytical solutions are frequently obtained by assuming that the equilibrium direction of the magnetization coincides with the direction (θ_H,ϕ_H) of the external magnetic field, i.e.,

$$\theta_0 = \theta_H, \text{ and } \phi_0 = \phi_H \quad (3)$$

However, it is important to point out that while this assumption may be valid along high-symmetry directions, it is generally not a good approximation even for large external fields when the external magnetic field is applied at an arbitrary angle (see the discussion in Sec. IV B 1). If one further assumes that the external magnetic field is applied in the plane of the film ($\theta_H = 90°$) and that the easy axis of the uniaxial anisotropy coincides with the easy direction of the exchange bias effect ($\phi_u = \phi_{\rm eb} = 0$), one has for the dispersion relation (see for example reference [26]):

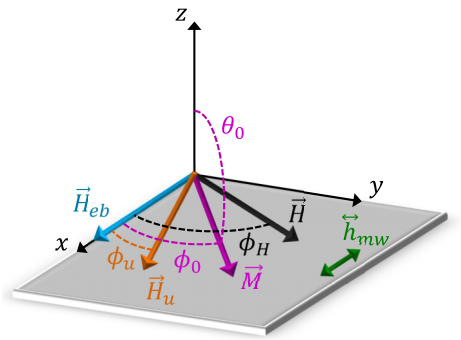

FIG. 1. Sketch of the geometry, where the exchange bias field $\vec{H}_{\rm eb}$ serves as a reference direction. The static external magnetic field $\vec{H}$ is applied in the film plane at an angle ϕ_H, with the microwave field $\vec{h}_{\rm mw}$ also applied in the film plane, but perpendicular to $\vec{H}$. Also shown is the magnetization $\vec{M}$ with equilibrium orientation (θ_0,ϕ_0) and the easy axis of the (in-plane) uniaxial anisotropy field $\vec{H}_u$, which is shown at an angle ϕ_u relative to the exchange bias direction.

$$\left(\frac{\omega}{\gamma}\right)^2 = [4\pi M_{\rm eff} + H_u\cos^2(\phi_H) + H_{\rm res} + H_{\rm eb}\cos(\phi_H)] \cdot [H_u\cos(2\phi_H) + H_{\rm res} + H_{\rm eb}\cos(\phi_H)] \quad (4)$$

in which $4\pi M_{\rm eff}$ is the effective magnetization (the sum of demagnetizing field and the perpendicular interfacial anisotropy field), $H_{\rm res}$ is the resonance field, and ϕ_H is the azimuthal angle of the applied static magnetic field with respect to the exchange bias direction.

When the external magnetic field is applied parallel ($\phi_H = 0°$) and antiparallel ($\phi_H = 180°$) to the exchange bias direction, Eq. (4) results in:

$$f = \frac{\gamma}{2\pi}\sqrt{[4\pi M_{\rm eff} + H_u + H_{\rm res} \pm H_{\rm eb}]\cdot[H_u + H_{\rm res} \pm H_{\rm eb}]} \quad (5)$$

where the positive (negative) sign corresponds to the parallel (antiparallel) orientation. For these two configurations, the external magnetic field is applied along high-symmetry directions of the system, and thus for sufficiently large fields, the magnetization will be aligned with the field direction. Therefore, this equation can be used to fit broadband FMR data to extract the exchange bias field, the uniaxial anisotropy field, the effective magnetization, and the gyromagnetic ratio.

Similarly, one can obtain an approximation for the in-plane angular dependence, which, for exchange-biased systems with a uniaxial anisotropy in the in-plane configuration, is commonly given as [8,27]:

$$H_{\rm res} = H_0 + H_{\rm eb}\cos(\phi_H) + H_u'\cos(2\phi_H) \quad (6)$$

where H_0 is the resonance field for the measurement microwave frequency in the absence of a unidirectional and

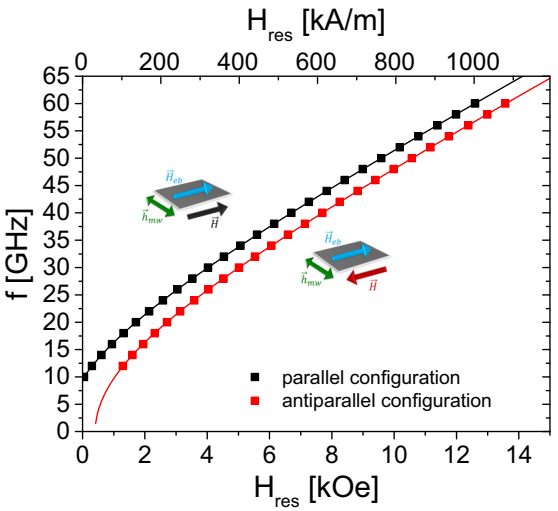

FIG. 2. Microwave frequency f versus resonance field $H_{\rm res}$ (Kittel plot) for a 6 nm CoFe exchange-biased layer. Black (red) symbols show broadband FMR data with the external magnetic field applied parallel (antiparallel) to the exchange bias direction. The corresponding solid lines are the result of a simulataneous fit to the Kittel Eq. (6) for both orientations.

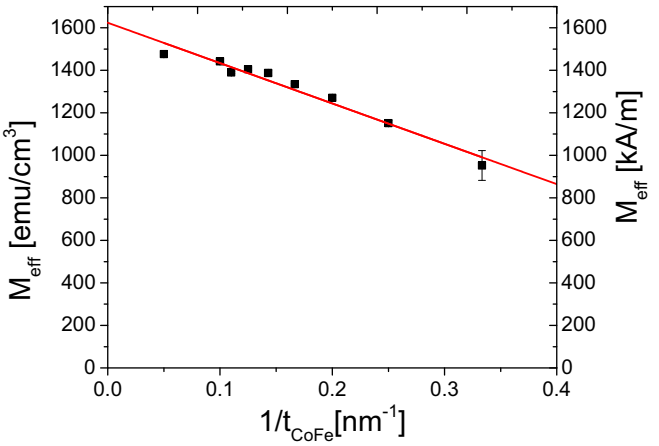

FIG. 3. Effective magnetization $M_{\rm eff}$, determined using broadband ferromagnetic resonance data, as a function of the inverse CoFe film thickness $t_{\rm CoFe}$. The red line is a linear fit to the experimental data.

uniaxial anisotropy. The use of an analytic function to describe the angular dependence of the resonance field can simplify the data analysis significantly. However, as will be shown below, this approximation can cause systematic variations of the residuals of the fit to experimental in-plane rotation data. In particular, we will show that the underlying approximations that were used to derive Eq. (6) will lead to the appearance of an unphysical threefold symmetry in the residuals of the fit to $H_{\rm res}$ vs. ϕ_H data. We further would like to point out that the parameter $H_u{}'$ used in Eq. (6) to describe the uniaxial component of the resonance field should not be confused with the uniaxial anisotropy field H_u [28,29].

IV. MAGNETIC ANISOTROPIES

A. Broadband FMR characterization

For the exchange-biased thin films, broadband FMR measurements were performed with the static external magnetic field applied parallel and antiparallel to the exchange bias direction. As shown in Fig. 2 for a 6 nm CoFe layer, the field dependence of the resonance frequency is well described by Eq. (5). In this figure, we have fitted both data sets simultaneously to obtain a consistent set of fitting parameters that minimizes the sum of the squared residuals.

By using this approach, broadband FMR data can provide precise values for the effective magnetization, $M_{\rm eff}$, and the gyromagnetic ratio, γ [30]. As shown in Fig. 3, the effective magnetization for the samples in this series shows an inverse CoFe thickness dependence with a negative slope, indicative of an interfacial perpendicular anisotropy. Assuming that there is no bulk perpendicular anisotropy present in CoFe, one can determine the saturation magnetization from this graph as $M_S = 1625 \pm 25$ (emu/cm^3); this value is consistent with results obtained using vibrating sample magnetometry. The slope is proportional to the interfacial perpendicular anisotropy, which in this sample series is $K_i = 1.94 \pm 0.14$ (erg/cm^2). This interfacial perpendicular anisotropy is comparable to those reported for CoFeB/MgO systems [31,32]; for the samples investigated in this work, we cannot distinguish between the perpendicular anisotropy contributions from the IrMn interface and from the Ru interface. However, given the large interfacial anisotropy present in the films, it is likely that both interfaces contribute significantly.

It is worth noting that carrying out broadband FMR measurements only for two in-plane orientations will limit the accuracy of the extracted anisotropy field values. In particular, any misalignment of the exchange bias field direction of the sample relative to the applied field during measurement will result in inaccurate values for the exchange bias field $H_{\rm eb}$ and the uniaxial anisotropy field H_u. Furthermore, even if the external magnetic field is perfectly aligned with the exchange bias field direction, but the easy axis of the uniaxial anisotropy does not coincide with the exchange bias direction, i.e., $\phi_u \neq 0$, the uniaxial anisotropy field will be systematically underestimated, as one is only sensitive to the component along the exchange bias field direction. We also find that the fitting parameters are highly correlated, and thus the fit is not very sensitive to the value of the uniaxial anisotropy. With these limitations in mind, it is clear that a more exhaustive method is needed to extract precise values of the involved anisotropies. FMR measurements as a function of the in-plane angle of the applied magnetic field not only provide a way to extract the magnitude of the anisotropies, but they also enable us to test the underlying assumption of our analysis, i.e., that the easy axis of the uniaxial anisotropy is aligned along the exchange bias direction.

B. In-plane angle–dependent characterization

1. FMR measurements

We carried out FMR measurements as a function of the in-plane angle of the applied field ϕ_H with respect to the exchange bias direction. As an example, the in-plane dependence of

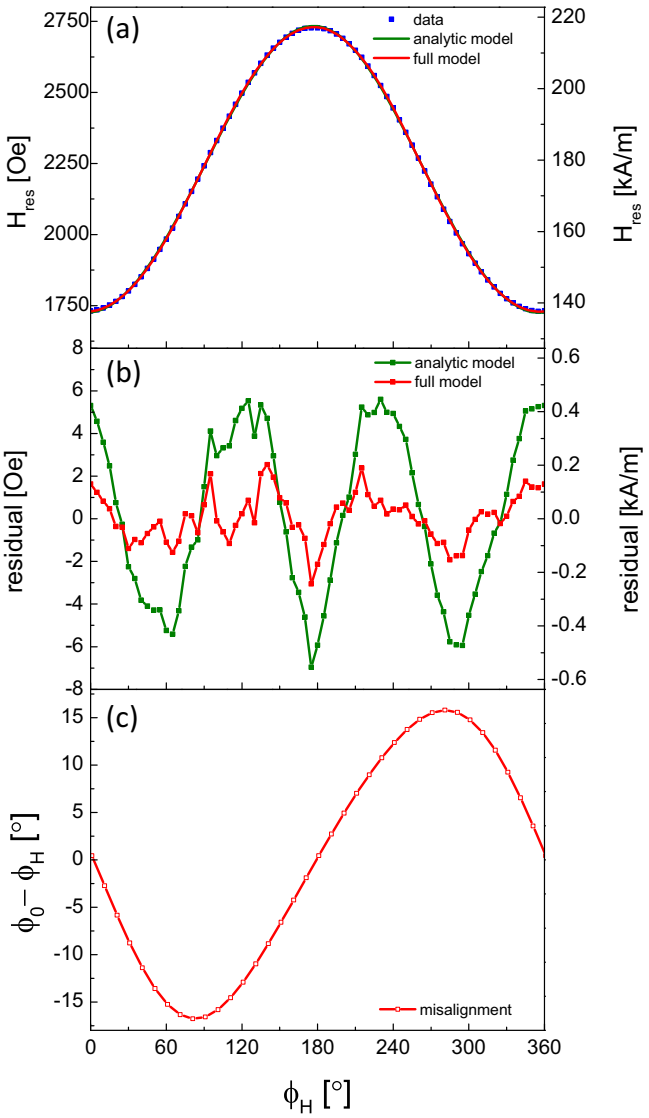

FIG. 4. Dependence on the in-plane angle of the applied field ϕ_H of (a) the resonance field H_{res} of a 6 nm CoFe exchange-biased layer, where the figure includes the experimental data (blue symbols), a fit using the analytic model (green line), and a fit using the full model (red line), (b) the residuals of the fit using the analytical model (green line and symbols) and the full model (red line & symbols), and (c) the misalignment of the in-plane angle of the magnetization ϕ_0 from the direction of the applied field ϕ_H calculated using the full model.

the resonance field measured at a microwave frequency of 20 GHz for a sample with a CoFe thickness of 6 nm is shown in Fig. 4(a). In this figure, a fit of the experimental data using the analytic model of Eq. (6) is shown as a green line. The full model based on Eq. (1), and minimizing the free energy to obtain the equilibrium orientation of the magnetization, is shown as a red line. At first glance, both fits appear to reasonably describe the experimental data, as on the scale of Fig. 4(a) both models are difficult to distinguish. However, closer inspection of the residuals for both fits, as shown in Fig. 4(b), reveals that the use of Eq. (6) leads to systematic deviations that show a threefold symmetry. While there have been prior reports of a threefold anisotropy contribution in exchange bias systems [33], for the systems investigated in the current study, the threefold symmetry of the residuals is a result of the assumptions made to arrive at Eq. (6), in particular, the assumption that the magnetization is aligned with the direction of the applied field. In Fig. 4(c), the difference between the magnetization angle ϕ_0 and the applied field angle ϕ_H, calculated using the full model, is shown, revealing misalignments as large as 15 degrees. As can be seen in Fig. 4(b), using the full model results in residuals that do not show any clear angular dependence.

In order to verify that the threefold symmetry in the residuals is solely an artifact of the analytical model, we simulated the in-plane angular dependence of the resonance field using the full model and subsequently tried to fit these data using Eq. (6). These simulations also reveal that it is the presence of both the exchange bias field and the uniaxial anisotropy that lead to this apparent threefold symmetry. In the limiting case with no exchange bias field, the residuals show a fourfold symmetry. We would also like to point out that while the uniaxial contribution to the resonance field H_u' in Eq. (6) is close to the value of the uniaxial anisotropy field H_u, the two values are not identical. A more accurate determination of the latter value, for a system without an exchange bias field, can be obtained by measuring the resonance field along the easy and hard directions and using Eq. (6) in reference [29]. In the limiting case with no uniaxial anisotropy, but with an exchange bias field, one can use Eq. (6) to fit the full model data with reasonable accuracy; in this case, the residuals again show a fourfold symmetry. A simulation and fit using Eq. (6) for the case of primary interest, where both an exchange bias field and a uniaxial anisotropy are present in the sample, is shown in Fig. 5. Here, the exchange bias field was chosen to be $H_{\text{eb}} = 500$ (Oe), and the uniaxial anisotropy field was set to $H_u = 200$ (Oe). By using a relatively large uniaxial anisotropy field, the limitations of the simplified model become more obvious. This can be seen by comparing Fig. 5(a) with Fig. 4(a). Due to the strong uniaxial anisotropy in Fig. 5(a), a clear minimum exists for the resonance around $\phi_H = 180°$ for the full model, whereas for a smaller uniaxial anisotropy, the deviations of the resonance field from a simple $\cos(\phi_H)$ dependence are more subtle; see Fig. 4(a). As pointed out earlier, the simplified model does not take into account the deviation of the equilibrium direction of the magnetization ϕ_0 from the direction of the applied field ϕ_H, which is shown in Fig. 5(c) and can reach 15 degrees, similar to the experimental case depicted in Fig. 4. A fit of the analytical model in Eq. (6) to the simulated data for the full model can therefore not capture the observed angular dependence. Because the fit attempts to minimize the sum of squares of the deviations, this leads to an underestimation of the resonance field parallel to the exchange bias direction and an overestimation of the resonance field antiparallel to the exchange bias direction. As can be seen in Fig. 5(a) and 5(b), over a full 360 degree rotation, there will be six points for which the fit and the full simulation intersect (dashed lines), which explains the observation that to first order, the symmetry of the residual is threefold. However, because the full model does not contain a threefold contribution to the free energy, this apparent threefold symmetry is an artifact of the assumptions made to derive Eq. (6), most notably the assumption that the magnetization is aligned with

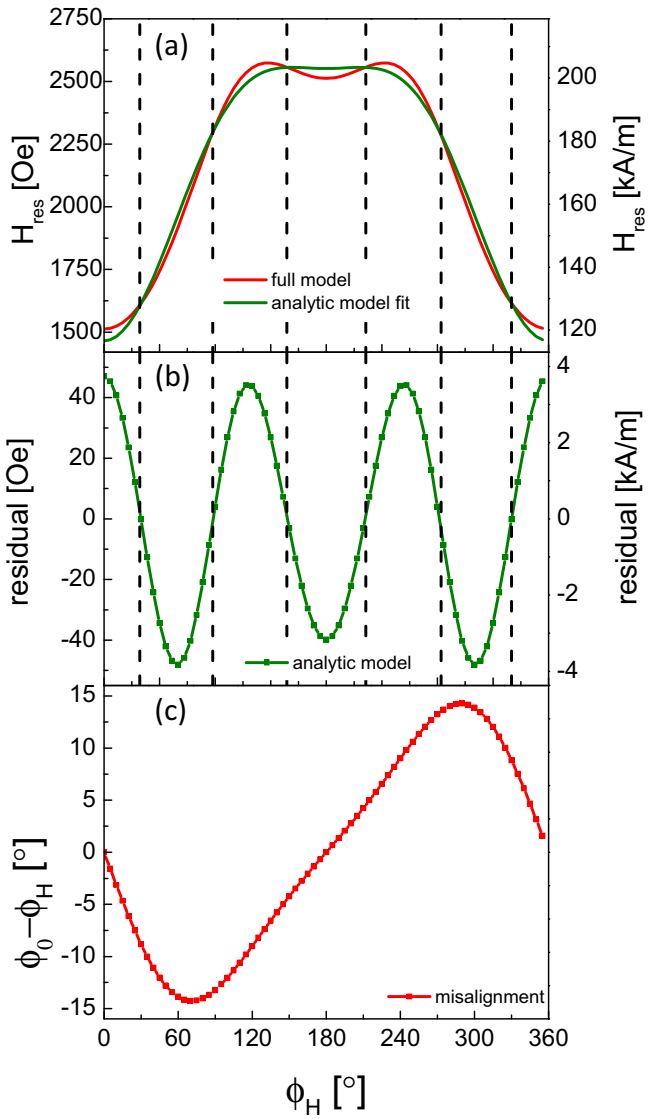

FIG. 5. Dependence on the in-plane angle of the applied field ϕ_H of (a) the resonance field H_{res}, where the red line is the result of the full model for $H_{\text{eb}} = 500$ (Oe) and $H_u = 200$ (Oe), and the green line is a fit of this data using Eq. (6), (b) the residuals of the fit, and (c) the misalignment of the equilibrium direction of the magnetization ϕ_0 from the direction of the applied field ϕ_H.

the external magnetic field. Thus, while at first glance, it may be tempting to add a threefold term to Eq. (6) similar to a Fourier series, our analysis shows that there is no physical significance to such a term, and one should instead use the full model to arrive at meaningful parameters.

By fitting the full model to the in-plane angle dependence of the resonance field for all samples, we were able to extract the exchange bias field H_{eb} and the uniaxial anisotropy field H_u. Furthermore, the angle ϕ_H of the easy axis of the uniaxial anisotropy was treated as a free fitting parameter. However, within the error margins, the easy axis of the uniaxial anisotropy is indeed parallel to the easy direction of the unidirectional anisotropy, which justifies our analysis of the broadband FMR data for which this was the assumption.

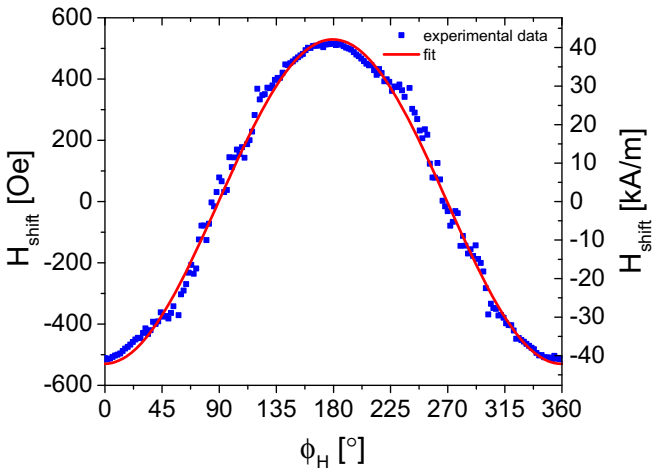

FIG. 6. Field shift H_{shift} of the magnetization reversal curves as a function of the in-plane angle ϕ_H of the applied field. Experimental data determined using the magneto-optic Kerr effect are shown as blue symbols, whereas the red line is a fit using $H_{\text{shift}}(\phi_H) = H_{\text{eb}}\cos(\phi_H)$.

2. *Quasistatic magnetometry*

We also carried out in-plane angle–dependent magnetization reversal measurements using the MOKE in longitudinal geometry. Measurements were carried out over a full 360 degree rotation, and the linear and quadratic Kerr-effect contributions were separated using a procedure described in detail in reference [34]. The linear Kerr-effect signal was subsequently analyzed to determine the two coercive fields for the increasing and decreasing field branches of the magnetization reversal. From this, the shift of the reversal curves was determined as a function of the in-plane angle ϕ_H of the applied field. As can be seen in Fig. 6 for a 6-nm-thick CoFe film, the angular dependence of the shift of the magnetization reversal curves is well described by a cosine dependence, i.e., $H_{\text{eb}}\cos(\phi_H)$, which is consistent with the unidirectional anisotropy in the films due to the exchange bias effect. While additional in-plane anisotropies in exchange bias films can lead to complex phase diagrams [10,11,34], and thereby to deviations from such a simple behavior, we find for the samples of this study that the additional in-plane uniaxial anisotropy is too small to have a significant influence on the angular dependence of the shift of the hysteresis curves. This is consistent with the results from the in-plane angle–dependent FMR measurements, which also indicated that the uniaxial anisotropy field is small compared to the exchange bias field for all samples of this series.

In summary, the exchange bias field that is extracted from the magnetization reversal curves agrees well with the value determined from FMR data; see Fig. 7. Due to the interfacial nature of the exchange bias effect, the exchange bias field is expected to scale with the inverse of the thickness of the ferromagnetic layer [7,18,35], which is confirmed in Fig. 7. From the slope of this figure and the saturation magnetization determined earlier, one can determine the interface energy per unit area [7,36,37], also called interfacial exchange coupling, $\Delta\sigma = M_S \cdot t_{\text{CoFe}} \cdot H_{\text{eb}}$, which enables a comparison with other exchange bias systems. For the interfacial exchange coupling, we obtain a value of $\Delta\sigma = 0.53 \pm 0.02$ (erg/cm^2), which

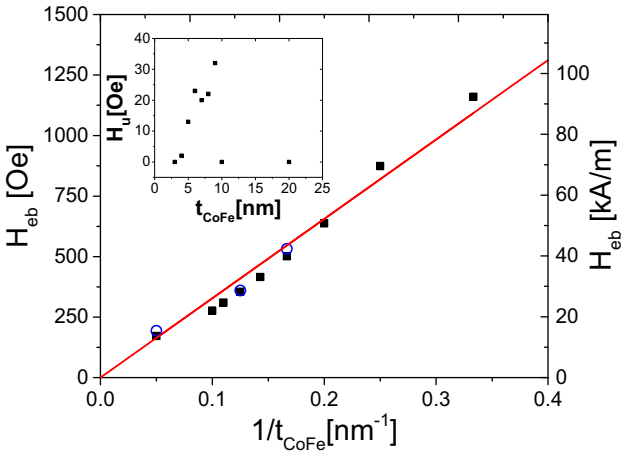

FIG. 7. Exchange bias field H_{eb} as a function of the inverse of the CoFe thickness t_{CoFe} as determined from ferromagnetic resonance data (black solid symbols) and magneto-optic Kerr effect data (blue open symbols). The red line shows a linear fit of the data. The inset shows the in-plane uniaxial anisotropy field as determined from ferromagnetic resonance data as a function of the CoFe thickness.

exceeds the values for all metallic antiferromagnets listed in Table 3 of reference [7] and is almost five times as big as the value reported in reference [38] for perpendicular CoFe/IrMn bilayers, which confirms the strong interfacial exchange coupling in our film series.

V. MAGNETIZATION RELAXATION

The linewidth of the FMR contains information about the magnetization relaxation and inhomogeneities in the samples. Using Suhl's approach [39], one can obtain an approximate expression for the peak-to-peak linewidth contribution due to Gilbert-type damping [25,40–42]:

$$\Delta H_{\mathrm{Gilbert}} \approx \frac{2}{\sqrt{3}} \frac{\alpha_{\mathrm{eff}}}{\gamma} \frac{\omega}{\cos(\phi_0 - \phi_H)} \tag{7}$$

where α_{eff} is the effective Gilbert-type damping parameter, and $\phi_0 - \phi_H$ is the misalignment between the magnetization and the external magnetic field. Under the assumption that the magnetization is perfectly aligned with the magnetic field and by including a zero frequency offset ΔH_0 that takes into account sample inhomogeneities, one has for the peak-to-peak linewidth [40,41,43]:

$$\Delta H = \Delta H_0 + \frac{2}{\sqrt{3}} \frac{\alpha_{\mathrm{eff}}}{\gamma} \omega \tag{8}$$

However, in thin films, two-magnon scattering can contribute significantly to the FMR linewidth measured with the magnetic field applied in the film plane. While the calculation of the two-magnon contribution $\Delta H_{2\text{-mag}}$ to the linewidth requires a quantitative model of the interfacial roughness, which is difficult to determine experimentally, under the assumptions for the roughness made by Arias and Mills, one

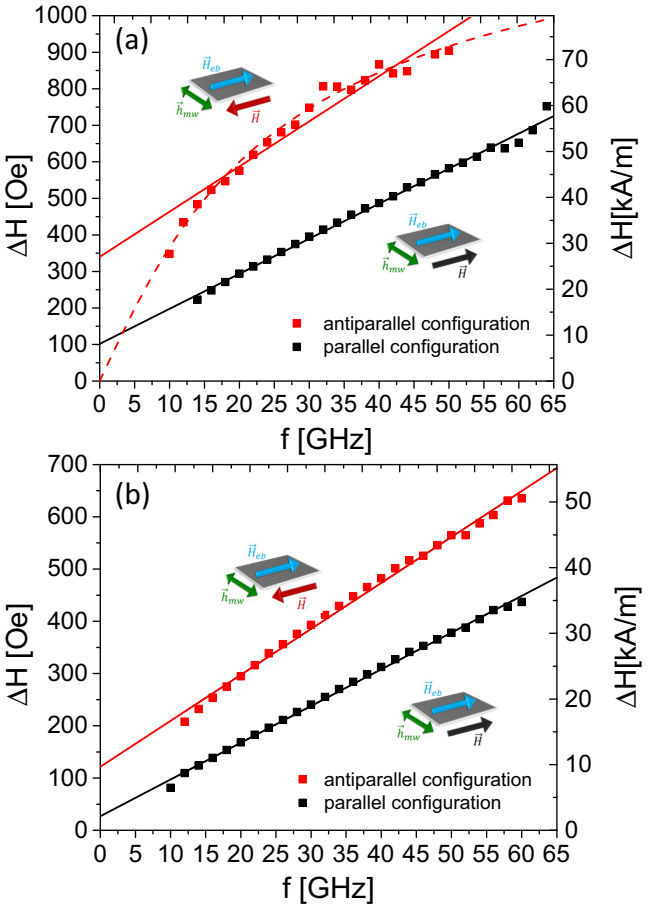

FIG. 8. Ferromagnetic resonance linewidth ΔH as a function of the microwave frequency f for a CoFe sample with a thickness of (a) $t_{\mathrm{CoFe}} = 4$ (nm) and (b) $t_{\mathrm{CoFe}} = 6$ (nm). The black (red) symbols represent broadband ferromagnetic resonance data measured with the field parallel (antiparallel) to the exchange bias direction. The solid lines show a fit of the data assuming Gilbert-type damping, Eq. (8), and the dashed line in (a) shows a fit of the data assuming two-magnon scattering as described by Eq. (9).

can obtain the following expression [44–46]:

$$\Delta H_{2\text{-mag}} = \Gamma(\omega) \arcsin \sqrt{\frac{\sqrt{\left(\frac{\omega_0}{2}\right)^2 + \omega^2} - \frac{\omega_0}{2}}{\sqrt{\left(\frac{\omega_0}{2}\right)^2 + \omega^2} + \frac{\omega_0}{2}}} \tag{9}$$

with $\omega_0 = \gamma 4\pi M_{\mathrm{eff}}$, and where $\Gamma(\omega)$ is the strength of the two-magnon scattering, which depends on the details of the interfacial roughness. If the two-magnon contribution is strictly interfacial, the scattering strength should scale like the inverse ferromagnetic film thickness squared [9,17]. Furthermore, the scattering strength depends only weakly on the microwave frequency [44].

Thus, one expects the ferromagnetic linewidth to be the sum of the contributions due to sample inhomogeneities, Gilbert-type damping, and two-magnon scattering:

$$\Delta H = \Delta H_0 + \Delta H_{\mathrm{Gilbert}} + \Delta H_{2\text{-mag}} \tag{10}$$

In Fig. 8(a), the FMR linewidth for a 4-nm-thick exchange-biased CoFe film is shown. For the measurements that were

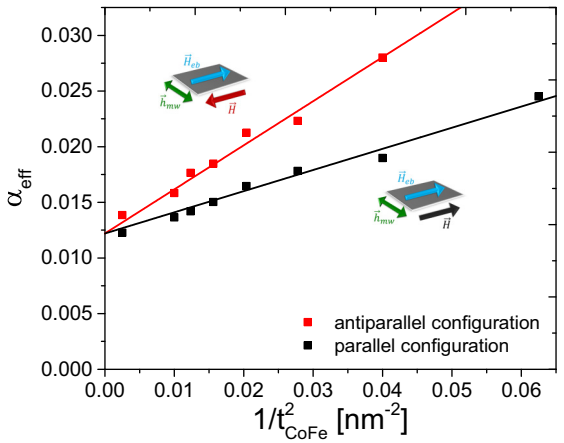

FIG. 9. Effective Gilbert-type damping parameter α_{eff} as a function of the square of the inverse CoFe thickness t_{CoFe}. The black (red) symbols represent damping parameters determined from broadband ferromagnetic resonance data measured with the field parallel (antiparallel) to the exchange bias direction. The solid lines show linear fits of the data.

carried out with the external magnetic field applied antiparallel to the exchange bias direction (red symbols), the frequency dependence of the linewidth is clearly nonlinear. The experimental data in this case can be fitted using the model for two-magnon scattering described by Eq. (9) with a frequency-independent scattering strength (dashed red line in Fig. 8(a)). However, we note that the nonlinearity of the two-magnon scattering is weak, and according to Eq. (9), for $\omega \ll \omega_0$, the two-magnon contribution is to a good approximation linear in frequency. This property of the two-magnon scattering prevents fitting of the experimental data, including all three contributions of the linewidth, because the fitting parameters in this case are highly correlated and not unique. Because the two-magnon scattering scales with t^{-2}_{CoFe}, its relative contribution to the overall FMR linewidth decreases quickly with increasing film thickness, as can be seen in Fig. 8(b). In this figure, the FMR linewidth for a 6-nm-thick exchange-biased CoFe film is shown as a function of the microwave frequency. In this case, the nonlinearity of the frequency dependence of the linewidth caused by the two-magnon scattering, while still noticeable, is not very pronounced. Because of the difficulties in separating the Gilbert-type damping contribution and the two-magnon scattering contribution to the linewidth, we therefore analyzed the data by neglecting the nonlinearity of the two-magnon contribution to the linewidth and instead fit the data using only the zero frequency offset ΔH_0 due to inhomogeneities and an effective Gilbert-type damping α_{eff}, which, in this approach, also includes the two-magnon contribution.

Accordingly, as shown in Fig. 9, the effective damping parameter scales approximately with the inverse ferromagnetic film thickness squared, indicating that two-magnon scattering is the dominant relaxation mechanism for the thinnest films of the series. This figure also shows clearly that the relaxation in these exchange-biased films is anisotropic and in particular is significantly larger when the magnetic field is applied antiparallel to the exchange bias direction compared to the parallel case. This suggests that the relaxation is unidirectional

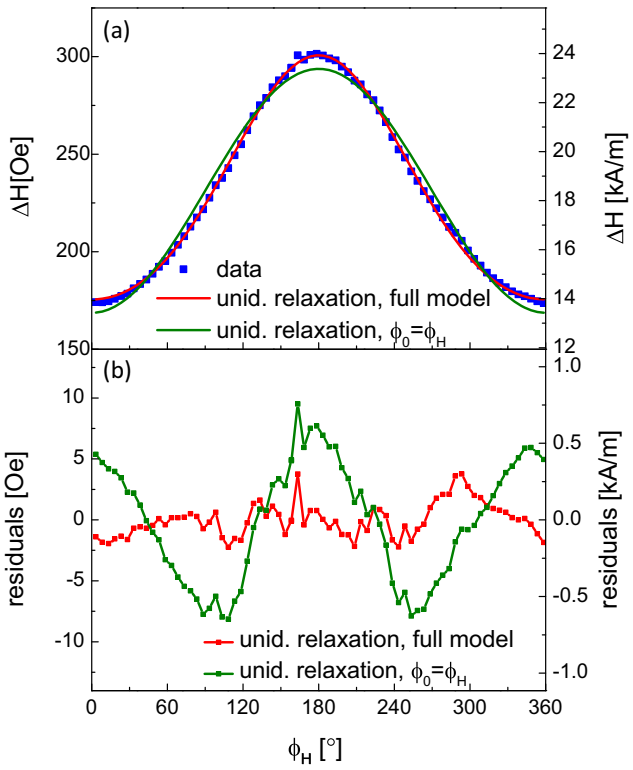

FIG. 10. (a) Peak-to-peak ferromagnetic resonance linewidth ΔH as a function of the in-plane angle ϕ_H of the applied field measured for a 6-nm-thick exchange-biased CoFe film at a microwave frequency of $f = 20$ (GHz). Experimental data are shown as blue symbols, where the red and green lines represent fits using a unidirectional relaxation described by Eq. (11) using the full model and assuming $\phi_0 = \phi_H$ respectively. (b) Residuals of the two different fits.

in nature, as had been reported previously for NiFe/FeMn exchange-biased structures [21].

To further investigate the unidirectional nature of the relaxation, we carried out in-plane angle–dependent measurements of the FMR linewidth at a fixed frequency, as shown in Fig. 10. Because the scattering strength of two-magnon scattering in thin films is determined by the perturbations at the interface, it will reflect the in-plane angular dependence of these perturbations [42,44,47–51]. In the case of exchange bias systems, one therefore expects the linewidth to show a unidirectional anisotropy as a function of the magnetization direction ϕ_0, i.e.,

$$\Delta H(\phi_H) = \Delta H_{\text{min}} + \frac{\Delta H_{\text{eb}}}{2}(1 - \cos\phi_0) \qquad (11)$$

Here, ΔH_{min} represents the minimal linewidth, measured parallel to the exchange bias direction. This term includes the Gilbert-type damping and isotropic contributions to the linewidth at the measurement frequency. The magnitude of the unidirectional contribution to the linewidth is characterized by the parameter ΔH_{eb}. Through the magnetization direction ϕ_0, the linewidth depends on the direction of the external magnetic field ϕ_H, which is varied in the experiment. If one assumes that the magnetization is aligned with the external magnetic field, Eq. (11) results in a simple cosine dependence of the linewidth with respect to the applied field direction. However,

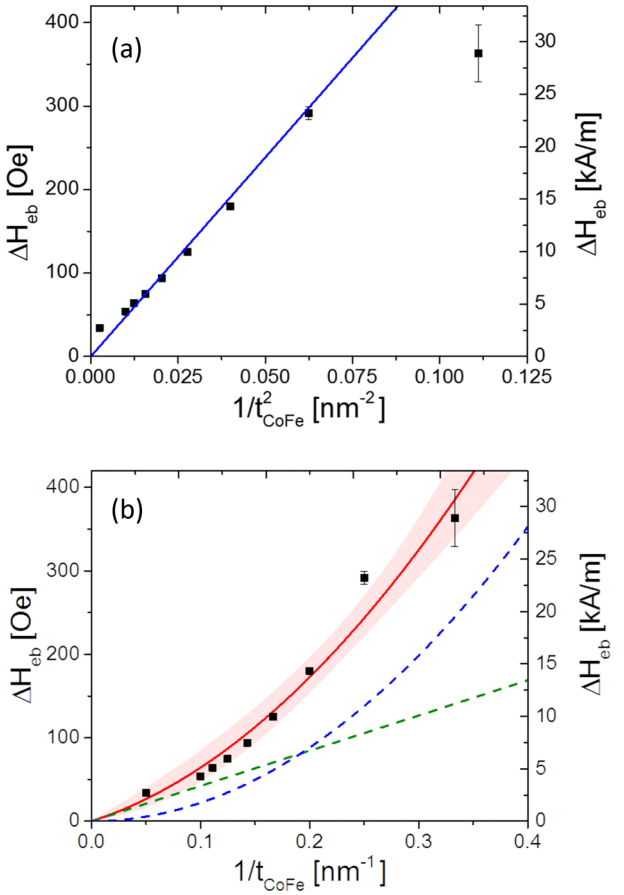

FIG. 11. Unidirectional linewidth contribution ΔH_{eb} determined from in-plane angle–dependent ferromagnetic resonance measurements. (a) Contribution is plotted as a function of $1/t_{\mathrm{CoFe}}^2$, where the blue line is a linear fit of the data with a vanishing unidirectional linewidth contribution for the bulk. (b) The same data shown as a function of the inverse CoFe thickness t_{CoFe}. The red line is a fit including a linear contribution (dashed green line) and quadratic contribution (dashed blue line) in the inverse film thickness. The red shaded area indicates the 95% confidence bands of the fit.

as discussed earlier, for the samples of the current study, this assumption is not a good approximation, given the large misalignments we observed (see Fig. 4(c)). Correspondingly, an attempt to fit the experimental data with a simple cosine dependence results in a systematic twofold symmetry of the residuals (Fig. 10(b)), which could lead to the erroneous introduction of an additional relaxation mechanism with this symmetry. In contrast, the full model discussed earlier, which minimized the free energy of the system to obtain the magnetization direction, results in an excellent description of the experimental data using only two fitting parameters.

In Fig. 11(a), the magnitude of the unidirectional contribution to the linewidth ΔH_{eb} determined for all samples by fitting the experimental data using Eq. (11) is shown as a function of the inverse square of the CoFe thickness t_{CoFe}. If the unidirectional linewidth contribution were solely caused by a strictly interfacial two-magnon scattering, one would expect it to be proportional to $1/t_{\mathrm{CoFe}}^2$. This is because, in this case, the two-magnon scattering scales with the square of the scattering potential, which is proportional to the inverse of the ferromagnetic film thickness [9,17,18,21]. However, the blue fit curve in Fig. 11(a), which uses this relationship, results in a poor description of the data. In Fig. 11(b), we have therefore included an additional unidirectional contribution to the linewidth that scales with the inverse film thickness to fit the data. As can be seen in the figure, this results in a better description of the data. The fit also indicates that for films thinner than approximately 5 nm, the two-magnon contribution is stronger than the contribution that scales with the inverse CoFe film thickness, whereas for thicker films, the situation is reversed. Besides its scaling with the inverse square of the CoFe film thickness, the two-magnon scattering contribution is also expected to lead to a nonlinear frequency dependence of the linewidth, which, as previously discussed, was observed to be significantly stronger for thinner films (Fig. 8). We therefore conclude that the samples investigated in this study show strong evidence for the presence of a unidirectional contribution to the relaxation in exchange-biased films that is not caused by strictly interfacial two-magnon scattering.

While the possibility of unidirectional relaxation mechanisms involving conduction electrons at the interface with the antiferromagnet has been discussed in reference [21], more theoretical work is needed to obtain a quantitative description.

VI. SUMMARY

We have carried out broadband FMR characterization of a series of IrMn/CoFe exchange-biased bilayers. In addition to a strong exchange bias effect, our results show a significant reduction of the effective magnetization of the CoFe films with decreasing film thickness, caused by the presence of a strong interfacial perpendicular anisotropy. For in-plane angle–dependent FMR measurements, we have shown that an analytical model that is commonly used to describe these kind of data has limitations regarding the extraction of anisotropies and introduces artifacts that could be misinterpreted as an additional threefold anisotropy. However, the full model, which properly minimizes the free energy of the system, enables a precise determination of the exchange bias field and a small in-plane uniaxial anisotropy that is also present in these bilayers. The results of our FMR characterization are in good agreement with results obtained using quasistatic magnetization reversal curves. The interface energy of the exchange bias effect in our sample series exceeds values previously reported for metallic antiferromagnets.

Our frequency-dependent and in-plane angle–dependent measurements of the FMR linewidth indicate a strong unidirectional contribution to the relaxation in the films. Part of this unidirectional relaxation can be attributed to two-magnon scattering at the CoFe interface with the antiferromagnet. However, the thickness dependence of the unidirectional linewidth contribution extracted from in-plane angle–dependent measurements strongly suggests the presence of an additional unidirectional relaxation mechanism, i.e., a unidirectional relaxation not caused by strictly interfacial two-magnon scattering.

ACKNOWLEDGMENTS

We would like to acknowledge support by National Science Foundation (NSF) CAREER Award No. 0952929 and by NSF CAREER Award No. 1452670.

[1] W. H. Meiklejohn and C. P. Bean, New magnetic anisotropy, Phys. Rev. **102**, 1413 (1956).

[2] W. H. Meiklejohn and C. P. Bean, New magnetic anisotropy, Phys. Rev. **105**, 904 (1957).

[3] S. Gider, B.-U. Runge, A. C. Marley, and S. S. P. Parkin, The magnetic stability of spin-dependent tunneling devices, Science **281**, 797 (1998).

[4] A. V. Khvalkovskiy, D. Apalkov, S. Watts, R. Chepulskii, R. S. Beach, A. Ong, X. Tang, A. Driskill-Smith, W. H. Butler, P. B. Visscher, D. Lottis, E. Chen, V. Nikitin, and M. Krounbi, Basic principles of STT-MRAM cell operation in memory arrays, J. Phys. D: Appl. Phys. **46**, 074001 (2013).

[5] E. Chen, D. Apalkov, A. Driskill-Smith, A. Khvalkovskiy, D. Lottis, K. Moon, V. Nikitin, A. Ong, X. Tang, S. Watts, R. Kawakami, M. Krounbi, S. A. Wolf, S. J. Poon, J. W. Lu, A. W. Ghosh, M. Stan, W. Butler, T. Mewes, S. Gupta, C. K. A. Mewes, P. B. Visscher, and R. A. Lukaszew, Progress and prospects of spin transfer torque random access memory, IEEE Trans. Magn. **48**, 3025 (2012).

[6] R. L. Stamps, Mechanisms for exchange bias, J. Phys. D: Appl. Phys. **33**, R247 (2000).

[7] J. Nogués and I. K. Schuller, Exchange bias, J. Magn. Magn. Mat. **192**, 203 (1999).

[8] J. C. Scott, Ferromagnetic resonance studies in the bilayer system $Ni_{0.80}Fe_{0.20}/Mn_{0.50}Fe_{0.50}$: Exchange anisotropy, J. Appl. Phys. **57**, 3681 (1985).

[9] R. D. McMichael, M. D. Stiles, P. J. Chen, and W. F. Egelhoff, Ferromagnetic resonance linewidth in thin films coupled to NiO, J. Appl. Phys. **83**, 7037 (1998).

[10] T. Mewes, H. Nembach, M. Rickart, S. O. Demokritov, J. Fassbender, and B. Hillebrands, Angular dependence and phase diagrams of exchange-coupled epitaxial $Ni_{81}Fe_{19}/Fe_{50}Mn_{50}(001)$ bilayers, Phys. Rev. B **65**, 224423 (2002).

[11] T. Mewes, H. Nembach, J. Fassbender, B. Hillebrands, J.-V. Kim, and R. L. Stamps, Phase diagrams and energy barriers of exchange-biased bilayers with additional anisotropies in the ferromagnet, Phys. Rev. B **67**, 104422 (2003).

[12] J. Fassbender, S. Poppe, T. Mewes, A. Mougin, B. Hillebrands, D. Engel, M. Jung, A. Ehresmann, H. Schmoranzer, G. Faini, K. J. Kirk, and J. N. Chapman, Magnetization reversal of exchange bias double layers magnetically patterned by ion irradiation, Phys. Status Solidi A **189**, 439 (2002).

[13] H. S. Cho, C. Hou, M. Sun, and H. Fujiwara, Characteristics of 360°-domain walls observed by magnetic force microscope in exchange-biased NiFe films, J. Appl. Phys. **85**, 5160 (1999).

[14] J. McCord, R. Schäfer, R. Mattheis, and K.-U. Barholz, Kerr observations of asymmetric magnetization reversal processes in CoFe/IrMn bilayer systems, J. Appl. Phys. **93**, 5491 (2003).

[15] J. McCord and S. Mangin, Separation of low- and high-temperature contributions to the exchange bias in $Ni_{81}Fe_{19}$-NiO thin films, Phys. Rev. B **88**, 014416 (2013).

[16] W. Stoecklein, S. S. P. Parkin, and J. C. Scott, Ferromagnetic resonance studies of exchange-biased Permalloy thin films, Phys. Rev. B **38**, 6847 (1988).

[17] S. M. Rezende, A. Azevedo, M. A. Lucena, and F. M. de Aguiar, Anomalous spin-wave damping in exchange-biased films, Phys. Rev. B **63**, 214418 (2001).

[18] S. M. Rezende, M. A. Lucena, A. Azevedo, F. M. de Aguiar, J. R. Fermin, and S. S. P. Parkin, Exchange anisotropy and spin-wave damping in CoFe/IrMn bilayers, J. Appl. Phys. **93**, 7717 (2003).

[19] S. Riedling, M. Bauer, C. Mathieu, B. Hillebrands, R. Jungblut, J. Kohlhepp, and A. Reinders, In-plane anomalies of the exchange bias field in $Ni_{80}Fe_{20}/Fe_{50}Mn_{50}$ bilayers on Cu(110), J. Appl. Phys. **85**, 6648 (1999).

[20] D. L. Mills and S. M. Rezende, in *Spin Dynamics in Confined Magnetic Structures II*, edited by B. Hillebrands, and K. Ounadjela (Springer, Berlin, Heidelberg, 2003), p. 27.

[21] T. Mewes, R. L. Stamps, H. Lee, E. Edwards, M. Bradford, C. K. A. Mewes, Z. Tadisina, and S. Gupta, Unidirectional magnetization relaxation in exchange-biased films, IEEE Magn. Lett. **1**, 3500204 (2010).

[22] M. Ali, C. H. Marrows, M. Al-Jawad, B. J. Hickey, A. Misra, U. Nowak, and K. D. Usadel, Antiferromagnetic layer thickness dependence of the IrMn/Co exchange-bias system, Phys. Rev. B **68**, 214420 (2003).

[23] C. J. Oates, F. Y. Ogrin, S. L. Lee, P. C. Riedi, G. M. Smith, and T. Thomson, High field ferromagnetic resonance measurements of the anisotropy field of longitudinal recording thin-film media, J. Appl. Phys. **91**, 1417 (2002).

[24] N. Pachauri, B. Khodadadi, M. Althammer, A. V. Singh, B. Loukya, R. Datta, M. Iliev, L. Bezmaternykh, I. Gudim, T. Mewes, and A. Gupta, Study of structural and ferromagnetic resonance properties of spinel lithium ferrite ($LiFe_5O_8$) single crystals, J. Appl. Phys. **117**, 233907 (2015).

[25] C. K. A. Mewes and T. Mewes, in *Handbook of Nanomagnetism* (Pan Stanford, Singapore 2015), p. 71.

[26] P. G. Barreto, M. A. Sousa, F. Pelegrini, W. Alayo, F. J. Litterst, and E. Baggio-Saitovitch, Ferromagnetic resonance study of the misalignment between anisotropy axes in exchange-biased NiFe/FeMn/Co trilayers, Appl. Phys. Lett. **104**, 202403 (2014).

[27] H. Xi, K. R. Mountfield, and R. M. White, Ferromagnetic resonance studies of exchange biasing in $Ni_{81}Fe_{19}/Pt_{10}Mn_{90}$ bilayers, J. Appl. Phys. **87**, 4367 (2000).

[28] This can be seen, for example, by noting that in the limit of vanishing exchange bias field, i.e., $H_{eb} = 0$, Eq. (5) along the easy axis of the uniaxial anisotropy ($\phi_H = 0°$) simplifies to:

$$f = \frac{\gamma}{2\pi}\sqrt{[4\pi M_{\text{eff}} + H_u + H_{\text{res},0}] \cdot [H_u + H_{\text{res},0}]} \qquad \text{(f1)}$$

whereas along the hard axis of the uniaxial anisotropy ($\phi_H = 90°$) using Eq. (4), one has:

$$f = \frac{\gamma}{2\pi}\sqrt{[4\pi M_{\text{eff}} + H_{\text{res},90}] \cdot [-H_u + H_{\text{res},90}]} \qquad \text{(f2)}$$

From measurements of the resonance field at the same frequency f along the easy ($H_{\text{res},0}$) and hard axis ($H_{\text{res},90}$), one can therefore extract the uniaxial anisotropy field as follows:

$$H_u = \frac{-H_1 + \sqrt{H_1^2 - 4H_2}}{2} \qquad \text{(f3)}$$

with $H_1 = 2(H_{\text{res},0} + 4\pi M_{\text{eff}}) + H_{\text{res},90}$ and $H_2 = H_{\text{res},0} \cdot (H_{\text{res},0} + 4\pi M_{\text{eff}}) - H_{\text{res},90} \cdot (H_{\text{res},90} + 4\pi M_{\text{eff}})$. Note that this result is similar to reference [29], where an expression for H_u was derived assuming $H_u \ll 4\pi M_{\text{eff}}$. However, for Eq. (6) in the limit of vanishing exchange bias field, one has simply:

$$H_u' = \frac{H_{\text{res},90} - H_{\text{res},0}}{2} \qquad \text{(f4)}$$

[29] G. N. Kakazei, P. E. Wigen, K. Y. Guslienko, R. W. Chantrell, N. A. Lesnik, V. Metlushko, H. Shima, K. Fukamichi, Y. Otani, and V. Novosad, In-plane and out-of-plane uniaxial anisotropies

in rectangular arrays of circular dots studied by ferromagnetic resonance, J. Appl. Phys. **93**, 8418 (2003).

[30] J. M. Shaw, H. T. Nembach, T. J. Silva, and C. T. Boone, Precise determination of the spectroscopic g-factor by use of broadband ferromagnetic resonance spectroscopy, J. Appl. Phys. **114**, 243906 (2013).

[31] D. C. Worledge, G. Hu, D. W. Abraham, J. Z. Sun, P. L. Trouilloud, J. Nowak, S. Brown, M. C. Gaidis, E. J. O'Sullivan, and R. P. Robertazzi, Spin torque switching of perpendicular Ta|CoFeB|MgO-based magnetic tunnel junctions, Appl. Phys. Lett. **98**, 022501 (2011).

[32] J. Sinha, M. Hayashi, A. J. Kellock, S. Fukami, M. Yamanouchi, H. Sato, S. Ikeda, S. Mitani, S.-h. Yang, S. S. P. Parkin, and H. Ohno, Enhanced interface perpendicular magnetic anisotropy in Ta|CoFeB|MgO using nitrogen doped Ta underlayers, Appl. Phys. Lett. **102**, 242405 (2013).

[33] I. N. Krivorotov, C. Leighton, J. Nogués, I. K. Schuller, and E. D. Dahlberg, Relation between exchange anisotropy and magnetization reversal asymmetry in Fe/MnF_2 bilayers, Phys. Rev. B **65**, 100402 (2002).

[34] T. Mewes, H. Nembach, M. Rickart, and B. Hillebrands, Separation of the first- and second-order contributions in magneto-optic Kerr effect magnetometry of epitaxial FeMn/NiFe bilayers, J. Appl. Phys. **95**, 5324 (2004).

[35] Y. J. Tang, B. Roos, T. Mewes, S. O. Demokritov, B. Hillebrands, and Y. J. Wang, Enhanced coercivity of exchange-bias Fe/MnPd bilayers, Appl. Phys. Lett. **75**, 707 (1999).

[36] A. E. Berkowitz and K. Takano, Exchange anisotropy—a review, J. Magn. Magn. Mat. **200**, 552 (1999).

[37] A. P. Malozemoff, Random-field model of exchange anisotropy at rough ferromagnetic-antiferromagnetic interfaces, Phys. Rev. B **35**, 3679 (1987).

[38] J. Y. Chen, N. Thiyagarajah, H. J. Xu, and J. M. D. Coey, Perpendicular exchange bias effect in sputter-deposited CoFe/IrMn bilayers, Appl. Phys. Lett. **104**, 152405 (2014).

[39] H. Suhl, Ferromagnetic resonance in nickel ferrite between one and two kilomegacycles, Phys. Rev. **97**, 555 (1955).

[40] B. Heinrich, J. F. Cochran, and R. Hasegawa, FMR linebroadening in metals due to two-magnon scattering, J. Appl. Phys. **57**, 3690 (1985).

[41] Z. Celinski and B. Heinrich, Ferromagnetic resonance linewidth of Fe ultrathin films grown on a bcc Cu substrate, J. Appl. Phys. **70**, 5935 (1991).

[42] Y. V. Goryunov, N. N. Garif'yanov, G. G. Khaliullin, I. A. Garifullin, L. R. Tagirov, F. Schreiber, T. Mühge, and H. Zabel, Magnetic anisotropies of sputtered Fe films on MgO substrates, Phys. Rev. B **52**, 13450 (1995).

[43] T. D. Rossing, Resonance linewidth and anisotropy variation in thin films, J. Appl. Phys. **34**, 995 (1963).

[44] R. Arias and D. L. Mills, Extrinsic contributions to the ferromagnetic resonance response of ultrathin films, Phys. Rev. B **60**, 7395 (1999).

[45] R. Arias and D. L. Mills, Extrinsic contributions to the ferromagnetic resonance response of ultrathin films, J. Appl. Phys. **87**, 5455 (2000).

[46] D. L. Mills and R. Arias, The damping of spin motions in ultrathin films: Is the Landau–Lifschitz–Gilbert phenomenology applicable? Phys. B: Cond. Matt. **384**, 147 (2006).

[47] J. Lindner, K. Lenz, E. Kosubek, K. Baberschke, D. Spoddig, R. Meckenstock, J. Pelzl, Z. Frait, and D. L. Mills, Non-Gilbert-type damping of the magnetic relaxation in ultrathin ferromagnets: Importance of magnon-magnon scattering, Phys. Rev. B **68**, 060102 (2003).

[48] G. Woltersdorf and B. Heinrich, Two-magnon scattering in a self-assembled nanoscale network of misfit dislocations, Phys. Rev. B **69**, 184417 (2004).

[49] K. Lenz, H. Wende, W. Kuch, K. Baberschke, K. Nagy, and A. Jánossy, Two-magnon scattering and viscous Gilbert damping in ultrathin ferromagnets, Phys. Rev. B **73**, 144424 (2006).

[50] I. Barsukov, P. Landeros, R. Meckenstock, J. Lindner, D. Spoddig, Z.-A. Li, B. Krumme, H. Wende, D. L. Mills, and M. Farle, Tuning magnetic relaxation by oblique deposition, Phys. Rev. B **85**, 014420 (2012).

[51] H. Kurebayashi, T. D. Skinner, K. Khazen, K. Olejník, D. Fang, C. Ciccarelli, R. P. Campion, B. L. Gallagher, L. Fleet, A. Hirohata, and A. J. Ferguson, Uniaxial anisotropy of two-magnon scattering in an ultrathin epitaxial Fe layer on GaAs, Appl. Phys. Lett. **102**, 062415 (2013).